

Petrol, pellets, paint?

Sourcing anthropogenic lead pollution in Plum Island sediments via stable-isotope analysis

JAMES YUNZHANG HU

The University of Chicago

Chicago, IL 60637

Mentor: ANNE GIBLIN

The Ecosystems Center, Marine Biological Laboratory

Woods Hole, MA 02543

Semester in Environmental Science

Marine Biological Laboratory

Class of 2021

ABSTRACT

Human activity has released lead into ecosystems in many different configurations of manufactured product, including leaded petrol (gasoline), lead gunshot pellets (shot), and lead-based paints. Recently, very high lead contamination has been reported for the wetland areas around the Plum Island estuarine system. To constrain the potential sources of the lead in Plum Island, I analyzed the chemical composition of surficial and core samples of Plum Island sediments for their concentrations of Pb isotopes and organic matter content. I also measured concentrations of Zn and Cr. Because lead has four different stable isotopes whose ratios have been used to constrain possible lead sources through the endmember's reported unique isotopic fingerprints. I measured the lead isotope ratios to see if they are similar to those of a hypothesized endmember (i.e., gasoline, shot, or paints) to better understand the contribution by that endmember to local pollution. Therefore, I also conducted a review of the scientific literature to estimate the lead isotope ratios of the hypothesized endmembers. Overall, I found that surface lead concentrations were an order of magnitude lower than previously reported, with a mean concentration of $\sim 20 \mu\text{g g}^{-1}$ dry soil in the main regions studied and several localized spikes exceeding $100 \mu\text{g g}^{-1}$ dry soil. Lead concentrations correlated weakly with chromium and zinc concentrations, but organic matter content did not correlate meaningfully with heavy-metal concentrations. Core samples indicated a general increase in sediment lead content as depth increased, sometimes followed by a decrease, in line with the history of lead regulation in the United States. However, a comparison of sample and hypothesized lead isotope ratios yielded little meaningful information about the etiology of Plum Island lead pollution. The large discrepancy between sample ratios and the range of endmember ratios calls into question the

viability of isotope fingerprinting, in the absence of robust local data, as a technique for investigating the sources of ecosystem-scale pollution.

Key words: lead; lead isotope composition; lead etiology; Plum Island; Massachusetts.

INTRODUCTION

Background and Context of Global Lead Pollution

The bulk of lead on Earth is contained in the lithosphere, at $\sim 5 \cdot 10^{19}$ g Pb, of which only minute portions naturally weather into sediments and soils or are released via volcanic emission. The release of lead to the biosphere and to ecosystems, through atmospheric and other sources, is therefore nearly entirely due to anthropogenic activity. Human use of lead began in prehistorical times for purposes both constructive (e.g., pottery and smelting) and destructive (e.g., intentional poisoning) (Svenberg 2000). The 20th century saw the domination of lead release into the atmosphere by the combustion of tetraethyllead-lined petrol (gasoline), a technology invented in the 1920s and phased out in automobiles over the last half-century in the United States and the rest of the world (Nriagu and Pacyna 1988; Weiss et al. 2007). Despite precipitous drops in atmospheric lead emissions across the world due to the general phase-out of leaded gasoline (Fiella and Bonet 2017), other sources of lead (including lead-based paint in urban areas and lead gunshot pellets, or shot, in rural areas) continue threaten the health of humans and ecosystems. Global environmental health issues due to lead pollution are therefore far from resolved (Ericson et al. 2017; Nriagu et al. 1995).

Lead is a neurotoxic heavy metal with detrimental effects on human and ecosystem health. With no known biological function in animals, lead harms virtually every major organ system by generating reactive oxygen species that damage biomolecules, impeding DNA transcription as well as the activity of enzymes (Flora et al. 2012; Wani et al. 2015). Lead

exposure in early childhood also severely impedes cognitive ability while boosting impulsiveness and aggression (Reyes 2015), and is potentially associated with criminality later in life (Denno 1990; Needleman et al. 1996). In practice, lead exposure represents a two-fold human threat: firstly, to public health and wellbeing worldwide and, secondly, to the Global South's economic development. Economists have estimated that lead exposure potentially costs low- and middle-income countries ~\$977 billion annually (Attina and Trasande 2013).

The effect of lead toxicity on animal, plant, and ecosystem health is also well-characterized. The United States EPA (2005) issued guidelines indicating that lead poses a risk to birds, mammals, plants, and soil invertebrates, in ascending order of safe threshold for lead concentration. Examples of lead poisoning in agricultural, natural, and laboratory settings abound. In animals, lead has fatally poisoned horses and cattle near a smelter (Hammond and Aronson 2006), has been shown to be toxic to mangrove microorganisms (Bayen 2012), and caused the deaths of at least 10,000 swans across 14 countries during a two-decade period near the height of atmospheric lead levels (Blus 1994). Even at trace levels considered permissible by the World Health Organization and the Food and Agriculture Organization of the United Nations, lead pollution is deleterious to certain terrestrial invertebrates (Monchanin et al. 2021). Plants growing in lead-polluted soils also exhibit lead accumulation in tissues, lowered growth rates, and altered metabolisms (Nagajyoti et al. 2010; Mitra et al. 2020).

Lead Pollution in the Plum Island Estuarine System

This study was motivated by data from Kristen Jezycki's master's thesis (2019) suggesting that sediments in the Plum Island Sound estuary, since the early 20th century, have consistently exhibited anomalously high lead concentrations compared with other estuaries along the U.S. East Coast. Compared to the baseline represented by Kennebec in Maine and Cape Fear

in North Carolina, Plum Island was two orders of magnitude higher. While the reason for such high lead concentrations is likely a mixture of various anthropogenic sources, no study to date has attempted to verify this claim or characterize lead etiology in Plum Island.

A number of potential historical and present sources of lead potentially contribute to the Plum Island Sound estuarine system. First, a large number of rivers and streams flow into Plum Island Sound, all of which are likely carrying various amounts of differently sourced lead into the estuary. Potential sources could therefore abound in quantity, type, and geographical distribution. For example, more urban areas and areas affected by combined sewer overflows could have more lead from lead paint and industrial processes, while wildlife areas could be more affected by lead shot and the use of lead in fishing. All sites would receive atmospheric lead, which, as described above, has changed in composition and quantity over time.

Secondly, organic matter content can influence the composition of lead that reaches the estuary. River sediments with higher organic matter content tend to adsorb to heavy metals more effectively (Lin and Chen 1998), thus perhaps retaining lead more effectively in locally, potentially lowering the amount of contribution to estuarine lead pollution but exacerbating local ecosystem effects. Variations in organic matter composition along the rivers could potentially interfere with tracing efforts. If, for example, lead is preferentially retained at certain midstream sites, then data from those sites would be relatively less informative of what contributes to downstream pollution.

This study attempted to constrain the sources of lead in the estuary and drainage basin using isotope-analytical techniques. Lead occurs in four stable isotopic forms: ^{204}Pb with ~1.4% abundance, ^{206}Pb with ~24%, ^{207}Pb with ~22%, and ^{208}Pb with ~52% (Catanzaro et al. 1968). Among both natural and artificial configurations of lead, these isotopic forms are slightly

differentially enriched relative to the average and do not undergo significant post-depositional physical and chemical fractionation processes (Bollhöfer et al. 2001; Komárek et al. 2008). The isotopic composition of lead that is deposited therefore preserves the signature of its sources and can be used to forensically constrain potential sources. The isotopic fingerprinting of lead has been widely applied to diverse contexts across scientific disciplines (e.g., Gwizada and Smith 2000, Chen et al. 2016, Dietrich et al. 2021, Lima et al. 2004). For a review of lead isotopes in environmental science in particular, see Komárek et al. (2008).

In investigating lead isotopes, this study sought to achieve two main aims: to constrain the potential sources of recent lead pollution in Plum Island Sound by widely sampling surface sediments in the watershed, and to trace how this has changed through three time periods through successive depths of sediment core. Based on background knowledge about the region, I hypothesized that more recent depositions of lead contaminant were likely to be dominated by two sources: paint and shot. Lead-based paint, despite being banned, still washes off from the surfaces of old buildings, especially in densely populated, lower-income urban areas situated on the Merrimack River. Lead shot, although it has been banned in the Parker River National Wildlife Refuge, is still legal at the federal level in the United States and could still represent a significant source in the Martin Burns Wildlife Management Area on the upper reaches of the Rowley River.

Paint has been extensively documented as one of the leading sources of lead exposure in the U.S., with Lowell (on the Merrimack River) matching the profile of urban areas susceptible to lead paint exposure (Brown et al. 2016), while hunting practices involving lead shot are legal in northeastern Massachusetts, being only briefly banned in early 2017 before the ban was overturned by the U.S. Department of the Interior (U.S. Secretary of the Interior 2017).

Massachusetts contains no lead mines, which would otherwise probably constitute a significant source of contamination. I assumed that historical depositions, however, were likely to be dominated by leaded gasoline, which dominated mid-century atmospheric lead content and which was only phased out over the 1970s and 80s (Nadim et al. 2001).

METHODS

Study Site Observations and Sampling Procedure

For a visual representation of the sampling and chemical-analytic methods, see FIG. 1.

I selected 16 field sites (FIG. 2) in the Plum Island drainage basin, both to retrace the sampling sites selected by Jezycki (2019) and to obtain a maximally representative sample. These locations included areas of Stage Island Pool adjacent to the Sound; the banks of rivers (i.e., Parker, Merrimack, Ipswich, and Rowley) flowing into the estuary; the beaver ponds of the Martin Burns Wildlife Management Area upstream from the Parker River; and soils near houses known to have been painted with lead-based paints (i.e., the Pink House and Marshview).

At each of the 16 locations, I recorded the location coordinates and vegetation available. Then, I collected surficial samples using modified syringes with the tip removed and plunger tip loosened, such that the barrel served as a miniature corer. I collected three replicates per location to a depth of ~2 cm, and for each location aggregated the replicates into a labelled Ziploc bag. At five of the 16 locations, I used large corers to procure core samples to depths of 24 cm. In laboratory, to prepare each deep core for further analysis, I trisected each 24 cm core into three 8 cm segments: 0–8 cm, 8–16 cm, and 16–24 cm. To avoid having material from one location in the core contaminating other layers, I extruded each core, then discarded the outermost rim of each cylindrical core. I dried the 31 samples in an oven over two nights and homogenized each sample using a combination of a mortar and pestle, a Retsch ball mill, and a Wiley mill.

Laboratory Analysis of Sample Contents

For each dried, homogenized sample, I analyzed the carbon and nitrogen content using a Thermo Scientific Flash 2000 Carbon, Hydrogen, and Nitrogen (CHN) Analyzer, following the appropriate instructions for organic-rich soils (Semester in Environmental Science 2021).

To determine the concentration and isotopic composition of heavy metals, I prepared a leachate for each sample. I transferred approximately 1 g of each sample into a Falcon tube and leached each in 20 mL of 10% nitric acid overnight, mixing four times over the course of 15 hours. I then poured each leachate through filter paper inside a filtration funnel into a scintillation vial and diluted the leachate 50 fold, down to 2% concentration using a mixture of deionized water and nitric acid, such that nitric acid also reached 2% concentration. Separately, I prepared six mixed-metals standard solutions in 2% nitric acid (concentrations, in mg L⁻¹, of 0.02, 0.04, 0.08, 0.2, 0.4, and 0.8) containing lead, zinc-66, and chromium-52, in addition to one blank solution consisting of 2% nitric acid only.

I subsequently analyzed the standard solutions and leachates using a Thermo Scientific iCAP Qc Inductively Coupled Plasma Mass Spectrometer (ICP-MS). I ran the analysis in collisional kinetic energy discrimination (KED) mode using He gas and analyzed for the following identifiers (dwell times in parentheses): ⁵²Cr (0.05 s), ⁶⁶Zn (0.03 s), ²⁰⁴Pb (0.07 s), ²⁰⁶Pb (0.05 s), ²⁰⁷Pb (0.05 s), and ²⁰⁸Pb (0.03 s). To correct for the interference of ²⁰⁴Hg, I additionally analyzed for ²⁰⁰Hg (0.03 s). For each analysis, the machine performed 15 sweeps and 5 main runs at normal resolution.

Data Analysis

I converted ICP-MS output from count number to concentration by performing least-squares regression on the data for my standard solutions of known concentration and then applying the resultant slope and intercept to my samples of unknown concentration. I performed data processing using Microsoft Excel and used open-source software to perform all other computational and graphical processing. Specifically, I created data figures using NumPy 1.20.1 (Harris et al. 2020), Pandas 1.2.3 (McKinney 2010; Pandas Development Team 2020), and Matplotlib 3.3.4 (Hunter 2007) in Python 3; and produced maps using QGIS 3.10.7 (QGIS Development Team 2020).

I also used Past 4.08 (Hammer et al. 2001) to conduct multivariate principal component analysis (PCA) across multiple dimensions, including proportion carbon, isotope ratios, and concentrations. To pre-process data for multivariate PCA, I log-transformed all concentrations (adding one, then taking the base-10 logarithm), took the square root of proportion carbon, and took the square root of all ratios. Subsequently, I selected different combinations of dimensions by which to analyze patterns in my samples.

Literature Review of Representative Isotopic Ratios

Using Web of Science and Google Scholar, I performed searches for lead isotope data for the three primary materials of interest (gasoline, lead shot, and lead-based paints) and gathered relevant primary research studies that reported isotopic ratios in those materials. I then extracted, recorded, and averaged individual ratios of interest (e.g., $^{207}\text{Pb}/^{204}\text{Pb}$) reported by each study. For ratios omitted from studies, I calculated those values using other ratios (e.g., $^{208}\text{Pb}/^{207}\text{Pb}$ divided by $^{207}\text{Pb}/^{206}\text{Pb}$ yields $^{208}\text{Pb}/^{207}\text{Pb}$). Finally, I averaged the ratios reported by each study to obtain an average literature value for each material and calculated standard error among study averages.

RESULTS

The majority of the 16 sites I visited were saline wetland sites that exhibited a general abundance of *Spartina* species and to a lesser extent of *Distichlis spicata* and *Phragmites*. The exceptions were the Martin Burns Wildlife Management Area (henceforth “Martin Burns”) sites, near a freshwater beaver pond, where I took samples six, 11, and 16 (TABLE 1) and the sample from the Marshview Farm which was upland. At the five sites where I also took core samples, I did not identify subsurface vegetation.

The mean surficial lead concentration was $112.6 \mu\text{g g}^{-1}$ dry soil, albeit with great variability (FIG. 3). When excluding the four highest values (those of samples from Martin Burns, the Pink House, and Marshview), the mean concentration of lead in surficial samples was $18.3 \mu\text{g g}^{-1}$ dry soil. When the surficial samples were binned into regional categories, each region where multiple samples were taken had a mean standard error of $\pm 2.4 \mu\text{g g}^{-1}$ dry soil.

The mean surficial zinc-66 concentration was $4.4 \mu\text{g g}^{-1}$ dry soil, while zinc-66 levels were below detection (i.e., the count number was less than that of the trace metal-grade blanks) in the Martin Burns Wildlife Management Area, the Pink House, and Marshview Farm (FIG. 4). The mean standard error for zinc-66 concentration was $0.8 \mu\text{g g}^{-1}$ dry soil. The mean surficial chromium-52 concentration was $182 \mu\text{g g}^{-1}$ dry soil and was below detection at the Merrimack site. Excluding the two highest values (those of samples from Rowley and the Pink House, which were in excess of $500 \mu\text{g g}^{-1}$ dry soil), the mean concentration of chromium-52 in surficial samples was $17.3 \mu\text{g g}^{-1}$ dry soil.

Lead concentrations in core samples exhibited different depth profiles but with several commonly shared features (FIG. 6). The five cores uniformly showed higher mean lead concentrations than the surficial (0–2 cm) sample taken at the same site: the mean lead

concentration in the cores was $57.4 \mu\text{g g}^{-1}$ dry soil, while that in the surface samples was $18.0 \mu\text{g g}^{-1}$ dry soil. Four cores had comparably low lead concentrations, with a mean of $22.7 \mu\text{g g}^{-1}$ dry soil, in their bottommost (16–24 cm) segment. With a $211.9 \mu\text{g g}^{-1}$ dry soil concentration at 16–24 cm, Core D was the exception. The middle depths generally saw the highest lead concentrations, with Cores A and B peaking at 8–16 cm and Cores D (excluding its extremely high 16–24 cm value) and E peaking at 0–8 cm. Of the five cores, Core C was the only one with fairly uniform lead concentration by depth, with a standard error of only $\pm 1.2 \mu\text{g g}^{-1}$ dry soil.

Zinc-66 concentrations in core samples also exhibited highly variable depth profiles, with zinc-66 below detection in several samples (FIG. 7). While patterns of change in concentration by depth were not obvious, at each of the five sites, the corresponding 0–2 cm samples showed a lower zinc-66 concentration than the mean core zinc-66 concentration. However, Core D showed an increase in zinc-66 concentration from 0–8 cm to 0–2 cm (Sample 12). Overall, chromium-52 concentrations in core samples exhibited less variable depth profiles than either lead or zinc-66 (FIG. 8). Chromium-52 spikes in cores were rare, with only two instances, each occurring at a different depth. Excluding the two spikes, chromium-52 concentration generally decreased with depth. Zero-to-two cm samples uniformly showed lower chromium-52 concentrations than at any other depth in the corresponding cores.

The proportion carbon by weight ranged from 4.3% to 27.7% with a mean of 13.1% and did not meaningfully correlate with the concentrations of lead, zinc-66, or chromium-52 (FIG. 9). Zinc-66 and chromium-52 concentrations did, however, somewhat correlate with lead concentrations, although the relationship is weaker at lower lead concentrations (FIG. 10).

In my literature search, I determined that 14 research studies provided adequate data for determining endmember lead isotope composition (TABLE 2). Synthesizing these data, I found

that leaded gasoline, lead shot, and lead-based paint had, by and large, non-overlapping coverage ranges on $^{208}\text{Pb}/^{206}\text{Pb}$ versus $^{207}\text{Pb}/^{206}\text{Pb}$ plots and $^{207}\text{Pb}/^{204}\text{Pb}$ versus $^{206}\text{Pb}/^{204}\text{Pb}$ plots (FIG. 11). Paint and gasoline had the extreme-most values, while lead shot had intermediate values, in both plots.

ICP-MS analysis of samples indicated that, by some measures, the majority of samples had drastically different lead isotope ratios than those of presumed endmembers (FIG. 12). For example, the majority of samples had higher $^{208}\text{Pb}/^{206}\text{Pb}$ ratios than any endmembers, while most samples had lower $^{207}\text{Pb}/^{204}\text{Pb}$ ratios than any endmembers. Nevertheless, $^{207}\text{Pb}/^{206}\text{Pb}$ range of the endmembers and samples exhibited significant overlap. The degree and nature of clustering of sample lead isotope ratios by region also varied considerably (FIG. 13.). The degree of clustering was highest among Parker River samples and between the Martin Burns samples, while it was lower among other sample groups. Similarly, the isotope ratios of cores alone are highly varied (FIG. 14). The 0–8 cm, 8–16 cm, and 16–24 cm samples show no general direction of movement through depth (and hence time), and exhibit similar overall isotopic signatures as the surficial samples.

PCA of samples based on multiple dimensions demonstrated that most of the variability among samples could be explained by, first, differences in zinc-66 concentration and, second, differences in chromium-52 concentration (TABLE 3). The PCA scatter plot showed several notable outliers across the multiple dimensions of measurement, including samples 6 (Hellcat Inside) in the Sound region, seven (Pink House), and 14 (Perleys Marina) by the Rowley River (FIG. 15).

DISCUSSION

Spatiotemporal Patterns in Lead Pollution in the Plum Island Estuarine System

Including sites like those in Martin Burns, surficial samples overall showed great variation in lead and chromium. However, five main regions of the study (Parker, Sound, Merrimack, Ipswich, and Rowley) showed very similar mean lead and zinc concentrations. These five sites, all near bodies of water, were particularly tightly constrained in terms of lead, clustering at $\sim 20 \mu\text{g g}^{-1}$ dry soil, suggesting that high levels of lead contamination in the Plum Island estuarine system could be highly localized, with limited downstream impacts. For instance, despite very high lead upstream lead pollution in Martin Burns, the Parker River surficial samples had similar levels of lead to all other regions. The same applies to the Pink House and Marshview, whose extremely high lead concentrations did not seem to correlate with any downstream spikes in the Sound or the Parker River.

Organic matter content, as proxied by proportion carbon, alone cannot adequately explain the highly localized nature of lead concentration spikes in the broader context of homogeneity. Possible alternative explanations include the source of pollution (e.g., atmospheric lead pollution could be more likely to cause relatively even spread of lead) and the relative rarity of lead concentration spikes in the area (i.e., because there are so few spikes, their impact does not accumulate). A spike in the concentration of one heavy metal does not generally correspond to that of another. Despite the slight correlation of zinc and chromium with lead concentrations, this lack of correspondence suggests that the sources of heavy-metal pollution in Plum Island could be idiosyncratic and largely unpatterned. For example, sample 14 shows an extremely high chromium concentration, likely a signature of chromium from bottom paint on boats docked at the local marina, but very low lead concentrations.

In core samples, lead concentrations generally show an initial increase with depth followed by a decrease, consistent with the widespread roll-out, then successful phase-out, of leaded gasoline across the United States over the last century. Evidence of the successful phase-out is particularly strong, with each of the five local surficial samples showing the lowest lead levels. The five cores exhibited spikes in lead concentration at different segments even though atmospheric lead ought to have been relatively uniform over the area, indicating that core depth is possibly not a reliable timestamp, perhaps due to different sedimentation rates. Alternatively, the difference in spike location could correspond with highly localized industrial contamination (e.g., the 16–24 cm spike in the Ipswich core) or different degrees of hunting in the area.

The average magnitude of lead pollution in Plum Island is a full order of magnitude short of the very high $259 \mu\text{g g}^{-1}$ level previously reported by Jezycki (2019). According to the EPA (2005), $259 \mu\text{g lead g}^{-1}$ dry soil would cause direct harm to plants, birds, and mammals. I used a weaker extraction than that used in Jezycki (2019). While this may explain part of the difference, it cannot explain the full extent of the discrepancy. In the absence of a proximate, identified source of lead pollution, and without a turning point in environmental regulation, it is also unlikely that lead concentrations would have changed since 2019; analyses of my surficial samples alone would have certainly detected spikes that occurred as recently as 2019. The reasons for the difference between the studies should be investigated. My data suggest the severity of recent lead pollution in Plum Island is far less. While lead pollution remains high enough to potentially cause harm to birds, it is insufficient to harm mammals or plants, in line with levels seen in other estuarine ecosystems on the East Coast of the United States.

Sourcing of Lead Pollution in the Plum Island Estuarine Ecosystem

The wide distribution of lead isotope ratios suggests the sourcing of lead pollution was, as expected, highly heterogeneous. Clear clustering does not emerge either from isotope ratios or from a multivariate PCA, suggesting that, even in the same region, different contributors of lead could be pulling the mean isotope ratio in different directions. In my core samples, isotope ratios do not exhibit any meaningful clustering at similar depths, despite the known historical phase-out of leaded gasoline that I had hypothesized would have left a visible isotopic imprint. This could be due to the unreliability of core depth as a proxy for time or, otherwise, could indicate that the signature of leaded gasoline used near Plum Island was not meaningfully different to those of other sources.

Ultimately, the drastically out-of-range (compared with endmember values) distribution of my data did not permit a mixing analysis of the relative contribution of the three candidate endmembers—leaded gasoline, lead shot, and lead-based paint—to the lead pollution. In general, my attempt to constrain the sources of Plum Island lead pollution met with challenges on many fronts. While one possibility was that the hypothesized endmembers did not account for most of the lead pollution, and that an external source was responsible for pollution, this seems unlikely.

At the core of the challenge was the lack of large amounts of high-quality data on local sources of lead. Although the literature review I conducted was able to relatively narrowly constrain the lead isotope ratios of the hypothesized endmembers, each study reported a wide range of data points. Chow and Earl (1972), for instance, reported $^{206}\text{Pb}/^{204}\text{Pb}$ values for leaded gasoline components ranging from 17.3 to 19.4, a difference that was not captured by the standard error of the mean of means of studies. The scarcity of accurate literature values representing the leaded gasoline characteristic of northeastern Massachusetts, combined with the

wide variety of possible lead ores that could have been added to leaded gasoline, used either presently in jet or boat fuel or historically in automobiles, probably further derailed the specific effort to define the expected endmember ratios for gasoline.

Further evidence for the inaccurate characterization of endmembers comes from ratios found at certain sites known to be contaminated by the endmembers in question. For example, as shown in FIG. 13(a), samples from the Pink House and Marshview that were known to have been painted with lead-based paint, contrary to expectations, exhibited significantly different isotope ratios to the presumed paint values. Also in the same figure are the ratios for the Martin Burns samples, which against expectations did not resemble those of the presumed lead shot values. Moreover, unexpectedly, core sample isotope ratios from the middle and bottom depths—despite higher lead concentrations, most likely due to leaded gasoline—did not approximate the expected range for gasoline (FIG. 14). Altogether, these disjunctions suggest that the lead isotope ratios from the literature review do not accurately characterize the actual endmembers that entered Plum Island. Differently formulated versions of the same product could have been manufactured using different lead ore sources with different isotopic ratios, and a correct selection of endmembers should be both space- and time-specific.

Implications for Lead Isotope Fingerprinting in Environmental Science

As observed by Duzgoren-Aydn and Weiss (2008), lead isotope fingerprinting as a technique has several inbuilt shortcomings, including its reliance on high-quality data and its assumption that candidate endmembers' isotope ratios are well-characterized within a narrow, non-overlapping ranges. They also argue that a high-quality, comprehensive database of relevant lead isotope ratios is necessary for meaningful ecosystem-level studies of lead source, because existing data are usually dated and specific to areas that do not necessarily share the same

endmember products as those of interest. Data about lead shot used in Alaska, for example, probably would not apply to a study on lead in Massachusetts. This study exemplifies a case in which the shortcomings of lead isotope fingerprinting inhibit its potential explanatory power.

To obtain more accurate endmembers, a future study could use dated core samples, rather than arbitrarily trisected core samples, to ascertain time stamps from which to derive plausible endmembers. Researchers could, for instance, use the spike in atmospheric lead in the 1970s to infer the isotopic signature of leaded gasoline. Even this method has limitations, however, because peaks in sources other than leaded gasoline are difficult to correlate with the historical time periods. In the most ideal scenario, researchers would be able to access actual endmember samples from which to obtain isotope ratios. As this is rarely feasible in larger-scale environmental research and over longer time periods, a comprehensive, time-stamped, and localized database containing endmember lead isotope ratios will likely be necessary for fruitful large-scale lead isotope research in the future.

ACKNOWLEDGEMENTS

I would like to thank my mentor, Anne Giblin, for her guidance and support throughout the project planning and execution process, as well as her rich knowledge of environmental chemistry and of the Plum Island Sound estuary, which partially motivated this research project. Thanks also to all the teaching faculty and staff at the Semester in Environmental Science, especially Kelsey Chenoweth, Emma Daily, Jade Fiorilla, and Rich McHorney, for helping me navigate the ins and outs of the laboratory; to Gretchen Swarr for her assistance in running analyses on the ICP-MS at the Clark Laboratory of the Woods Hole Oceanographic Institute; and to Javier Lloret for introducing me to multidimensional analysis software. This project would not have been possible without the generosity and help of these individuals.

LITERATURE CITED

- Adgate, J. L., G. G. Rhoads, and P. J. Liroy. 1998. The use of isotope ratios to apportion sources of lead in Jersey City, NJ, house dust wipe samples. *Science of the Total Environment* 221:171–180.
- Attina, T. M., and L. Trasande 2013. Economic costs of childhood lead exposure in low- and middle-income countries. *Environmental Health Perspectives* 121:1097–1102.
- Bayen, S. 2012. Occurrence, bioavailability and toxic effects of trace metals and organic contaminants in mangrove ecosystems: a review. *Environment International* 48:84–101.
- Binkowski, Ł. J., W. Meissner, M. Trzeciak, K. Izevbekhai, and J. Barker. 2016. Lead isotope ratio measurements as indicators for the source of lead poisoning in Mute swans (*Cygnus olor*) wintering in Puck Bay (northern Poland). *Chemosphere* 164:436–442.
- Blus, L. J. 1994. A review of lead poisoning in swans. *Comparative Biochemistry and Physiology Part C: Pharmacology, Toxicology and Endocrinology* 108:259–267.
- Bollhöfer, A., and K. J. R. Rosman. Isotopic source signatures for atmospheric lead: the Northern Hemisphere. *Geochimica et Cosmochimica Acta* 65:1727–1740.
- Brown, S. L., R. L. Chaney, and G. M. Hettiarachchi. 2016. Lead in urban soils: a real or perceived concern for urban agriculture? *Journal of Environmental Quality* 45:26–36.
- Chow, T. J., and J. L. Earl. 1972. Lead isotopes in North American coals. *Science* 176:510–511.
- Catanzaro, E. J., T. J. Murphy, W. R. Shields, and E. L. Garner. 1968. Absolute isotopic abundance ratios of common, equal-atom, and radiogenic lead isotopic standards. *Journal of Research of the National Bureau of Standards, Section A: Physics and Chemistry* 72:261–267.

- Denno, D. W. 1990. *Biology and Violence: From Birth to Adulthood*. Cambridge University Press, Cambridge, U.K.
- Duzgoren-Aydn, N. S., and A. L. Weiss. 2008. Use and abuse of Pb-isotope fingerprinting technique and GIS mapping data to assess lead in environmental studies. *Environmental Geochemistry and Health* 30:577–588.
- Ericson, B., H. Hu, E. Nash, G. Ferraro, J. Sinitsky, M. P. Taylor. 2017. Blood lead levels in low-income and middle-income countries: a systematic review. *Lancet Planetary Health* 5:e145–153.
- Finkelstein, M. E., Z. E. Kuspa, A. Welch, C. Eng, M. Clark, J. Burnett, and D. R. Smith. 2014. Linking cases of illegal shootings of the endangered California condor using stable lead isotope analysis. *Environmental Research* 134:270–279.
- Flora, G., D. Gupta, and A. Tiwari. 2012. Toxicity of lead: a review with recent updates. *Interdisciplinary Toxicology* 5:47–58.
- Hammer, Ø., D. A. T. Harper, and P. D. Ryan. 2001. PAST: paleontological statistics software package for education and data analysis. *Palaeontologia Electronica* 4:1–9.
- Hammond, P. B., and A. L. Aronson. 2006. Lead poisoning in cattle and horses in the vicinity of a smelter. *Annals of the New York Academy of Sciences* 111:595–611.
- Harris, C. R., K. J. Millman, S. J. van der Walt, R. Gommers, P. Virtanen, D. Cournapeau, E. Wieser, J. Taylor, S. Berg, N. J. Smith, R. Kern, M. Picus, S. Hoyer, M. H. van Kerkwijk, M. Brett, A. Haldane, J. Fernández del Río, M. Wiebe, P. Peterson, P. Gérard-Marchant, K. Sheppard, T. Reddy, W. Weckesser, H. Abbasi, C. Gohlke, and T. E. Oliphant. 2020. Array programming with NumPy. *Nature* 585:357–362.

- Hunter, J. D. 2007. Matplotlib: a 2D graphics environment. *Computing in Science & Engineering* 9:90-95.
- Hurst, R. W., T. E. Davis, and B. D. Chinn. 1996. The lead fingerprints of gasoline contamination: isotopic analysis of the lead additives in gasoline can improve estimates of the ages of leaks and spills. *Environmental Science and Technology* 30:304–307.
- Jezycki, K. E. 2019. Assessing heavy metal pollution in estuarine systems along the eastern United States in relation to land use land cover changes. Master's thesis, Villanova University, Villanova, Pennsylvania, U.S.A.
- Komárek, M., V. Ettler, V. Chrastný, and M. Mihaljevič. 2007. Lead isotopes in environmental sciences: a review. *Environment International* 34:562–577.
- Landmeyer, J. E., P. M. Bradley, and T. D. Bullen. 2003. Stable lead isotopes reveal a natural source of high lead concentrations to gasoline-contaminated groundwater. *Environmental Geology* 45:12–22.
- LeGalley, E., E. Widom, M. P. S. Krekeler, D. C. Kuentz. 2013. Chemical and lead isotope constraints on sources of metal pollution in street sediment and lichens in southwest Ohio. *Applied Geochemistry* 32:195–203.
- Lin, J.-G., and S.-Y. Chen. 1998. The relationship between adsorption of heavy metal and organic matter in river sediments. *Environment International* 24:345–352.
- McKinney, W. 2010. Data structures for statistical computing in Python. *Proceedings of the 9th Python in Science Conference* 445:56–61.
- Mitra, A., S. Chatterjee, A. V. Voronina, C. Walther, and D. K. Gupta. 2020. Lead toxicity in plants: a review. Pages 99–116 *in* D. K. Gupta, S. Chatterjee, and C. Walther, editors. *Radionuclides and Heavy Metals in the Environment*. Springer, Cham, Switzerland.

- Monchanin, C., J.-M. Devaud, A. B. Barron, and M. Lihoreau. 2021. Current permissible levels of metal pollutants harm terrestrial invertebrates. *Science of the Total Environment* 779:146398.
- Nagajyoti, P. C., K. D. Lee, and T. V. M. Sreekanth. 2010. Heavy metals, occurrence and toxicity for plants: a review. *Environmental Chemistry Letters* 8:199–216.
- Needleman, H. L., J. A. Riess, M. J. Tobin, G. E. Biesecker, J. B. Greenhouse. 1996. Bone lead levels and delinquent behavior. *JAMA* 275:363–369.
- Nriagu, J. O., M. L. Blankson, and K. Ocran. 1995. Childhood lead poisoning in Africa: a growing public health problem. *Science of the Total Environment* 181:93–100.
- Nriagu, J. O., and J. M. Pacyna. 1988. Quantitative assessment of worldwide contamination of air, water and soils by trace metals. *Nature* 333:134–139.
- Pandas Development Team. 2020. Pandas. Zenodo. <https://pandas.pydata.org/>
- Patel, M. M., H. Adrianne, R. Jones, J. Jarrett, J. Berner, and C. S. Rubin. 2008. Use of lead isotope ratios to identify sources of lead exposure in Alaska Natives. *International Journal of Circumpolar Health* 67:261–268.
- QGIS Development Team. 2020. QGIS Geographic Information System. Open Source Geospatial Foundation Project. <http://qgis.osgeo.org>
- Rabinowitz, M. B. 1987. Stable isotope mass spectrometry in childhood lead poisoning. *Biological Trace Element Research* 12:223–229.
- Reyes, J. 2015. Lead exposure and behavior: effects on antisocial and risky behavior among children and adolescents. *Economic Inquiry* 53:1580–1605.
- Semester in Environmental Science. 2021. Particulate carbon and nitrogen protocol: preparing and running samples for C and N analysis on the Thermo Scientific 2000. Pages arbitrary

- in K. H. Foreman and R. M. McHorney, editors. Green Binder: Methods. Marine Biological Laboratory, Woods Hole, Massachusetts, U.S.A.
- Smith, K. E., M. M. Shafer, D. Weiss, H. A. Anderson, P. R. Gorski. 2017. High-precision (MC-ICPMS) isotope ratio analysis reveals contrasting sources of elevated blood lead levels of an adult with retained bullet fragments, and of his child, in Milwaukee, Wisconsin. *Biological Trace Element Research* 177:33–42.
- Svanberg, F., R. Mateo, L. Hillström, A. J. Green, M. A. Taggart, A. Raab, and A. A. Meharg. 2006. Lead isotopes and lead shot ingestion in the globally threatened marbled teal (*Marmaronetta angustirostris*) and white-headed duck (*Oxyura leucocephala*). *Science of the Total Environment* 370:416–424.
- Svenberg, H. 2000. Lead poisoning in a historical perspective. *American Journal of Industrial Medicine* 38:244–254.
- Tsuji, L. J. S., B. C. Wainman, I. D. Martin, C. Sutherland, J.-P. Weber, P. Dumas, and E. Nieboer. 2008. The identification of lead ammunition as a source of lead exposure in First Nations: the use of lead isotope ratios. *Science of the Total Environment* 393:291–298.
- United States Environmental Protection Agency (EPA). 2005. Ecological soil screening levels for lead: interim final. EPA Office of Solid Waste and Emergency Response, Washington, District of Columbia, U.S.A. https://www.epa.gov/sites/default/files/2015-09/documents/eco-ssl_lead.pdf
- U.S. Secretary of the Interior. 2017. Order no. 3346: revocation of the United States Fish and Wildlife Service Director's order no. 219 (use of nontoxic ammunition and fishing

tackle). U.S. Department of the Interior, Washington, D.C., U.S.A.

https://www.doi.gov/sites/doi.gov/files/uploads/order_no._3346.pdf

- Viczián, M., A. Lásztity, and R. M. Barnes. 1990. Identification of potential environmental sources of childhood lead poisoning by inductively coupled plasma mass spectrometry: verification and case studies. *Journal of Analytical Atomic Spectrometry* 5:293–300.
- Wani, A. L., A. Ara, and J. A. Usmani. 2015. Lead toxicity: a review. *Interdisciplinary Toxicology* 8:55–64.

TABLE AND FIGURE LEGENDS

- TABLE 1 Description of sampling sites.
- TABLE 2 List of sources used to determine endmember lead isotope composition.
- TABLE 3 Summary of principal components analysis based on lead isotope ratios, zinc-66 and chromium-52 concentrations, and proportion carbon by weight.
- FIG. 1 Flow chart of project methods, created with BioRender.com.
- FIG. 2 Map of sampling sites in the Plum Island Sound estuary drainage basin.
- FIG. 3 Concentration of lead in surficial samples aggregated by region.
- FIG. 4 Concentration of zinc-66 in surficial samples aggregated by region.
- FIG. 5 Concentration of chromium-52 in surficial samples aggregated by region.
- FIG. 6 Concentration of lead in core samples by depth.
- FIG. 7 Concentration of zinc-66 in core samples by depth.
- FIG. 8 Concentration of chromium-52 in core samples by depth.
- FIG. 9 Proportion carbon by weight versus log-transformed heavy metal concentration.
- FIG. 10 Zinc-66 and chromium-52 concentrations versus lead concentration, all log-transformed.
- FIG. 11 Average endmember lead isotope ratios obtained from the scientific literature.
- FIG. 12 Measured lead isotope ratios juxtaposed to those of presumed endmembers.
- FIG. 13 Selected measured lead isotope ratios juxtaposed to those of other measurements and of presumed endmembers.
- FIG. 14 Measured lead isotope ratios of cores juxtaposed to those of presumed endmembers.
- FIG. 15 Principal components analysis based on lead isotope ratios, zinc-66 and chromium-52 concentrations, and proportion carbon by weight.

TABLES

TABLE 1. Description of sampling sites.

Label	Depth (cm)	Region	Description	Vegetation	Location (°N, °W)
1	0–2	Martin Burns	Outlet	Grassy, <i>Phragmites</i>	42.773, –70.923
2	0–2	Martin Burns	Draining Pond	Large grasses, <i>Typha</i>	42.773, –70.923
3	0–2	Parker	Middle Road	<i>S. patens</i> , <i>D. spicata</i>	42.759, –70.901
4	0–2	Sound	Stage Island Pool	<i>S. patens</i>	42.723, –70.785
5	0–2	Sound	Hellcat Outside	<i>S. alterniflora</i> , <i>S. patens</i> , <i>D. spicata</i>	42.740, –70.798
AT	0–8				
AM	8–16				
AB	16–24				
6	0–2	Sound	Hellcat Inside	<i>Phragmites</i>	42.741, –70.796
7	0–2	n/a	The Pink House	Grasses, <i>S. patens</i>	42.796, –70.830
8	0–2	Merrimack	Joppa Flats	<i>Phragmites</i> , <i>S. patens</i>	42.800, –70.848
BT	0–8				
BM	8–16				
BB	16–24				
9	0–2	Parker	Town Landing	<i>S. alterniflora</i>	42.763, –70.846
CT	0–8				
CM	8–16				

CB	16–24				
10	0–2	Parker	Stackyard Road	<i>S. patens</i>	42.744, –70.836
11	0–2	Ipswich	Ipswich Dam	n/a	42.684, –70.827
12	0–2	Ipswich	Marsh	<i>S. alterniflora</i>	42.716, –70.818
DT	0–8				
DM	8–16				
DB	16–24				
13	0–2	Ipswich	Greenwood Creek	<i>S. cynosuroides</i> , <i>Phragmites</i>	42.691, –70.818
14	0–2	Rowley	Perleys Marina	<i>S. alterniflora</i>	42.721, –70.859
15	0–2	Rowley	Rowley House	<i>S. alterniflora</i> , <i>D. spicata</i>	42.725, –70.856
ET	0–8				
EM	8–16				
EB	16–24				
16	0–2	n/a	Marshview	Foundation veg.	42.758, –70.892

TABLE 2. List of sources used to determine endmember lead isotope composition.

Leaded gasoline	Lead shot	Lead-based paint
Chow and Earl 1972	Adgate et al. 1998	LeGalley et al. 2013
Hurst et al. 1996	Binkowski et al. 2016	Rabinowitz 1987
Landmeyer et al. 2003	Finkelstein et al. 2014	Smith et al. 2017
	Patel et al. 2008	Viczián et al. 1990
	Smith et al. 2017	
	Svanberg et al. 2006	
	Tsuji et al. 2008	

TABLE 3. Summary of principal components analysis based on lead isotope ratios, zinc-66 and chromium-52 concentrations, and proportion carbon by weight.

Principal component	% variance	Primary loader (%)
1	65.0	$\log[\text{Zn } (\mu\text{g g}^{-1}) + 1]$ (98.2%)
2	22.1	$\log[\text{Cr } (\mu\text{g g}^{-1}) + 1]$ (96.5%)

FIGURES



FIG. 1. Flow chart of project methods, created with BioRender.com.

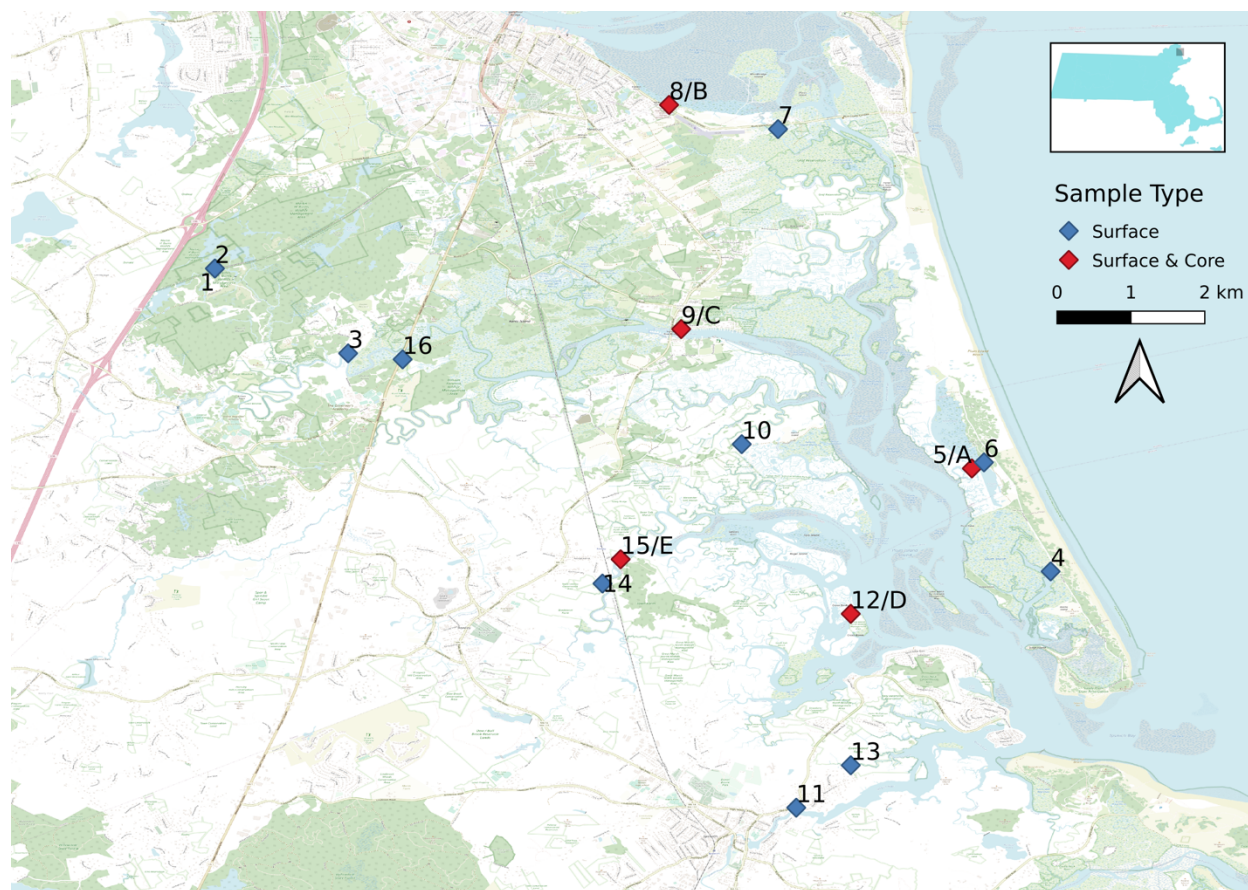


FIG. 2. Map of sampling sites in the Plum Island Sound estuary drainage basin. See TABLE 1 for correspondence between labels and sampling sites.

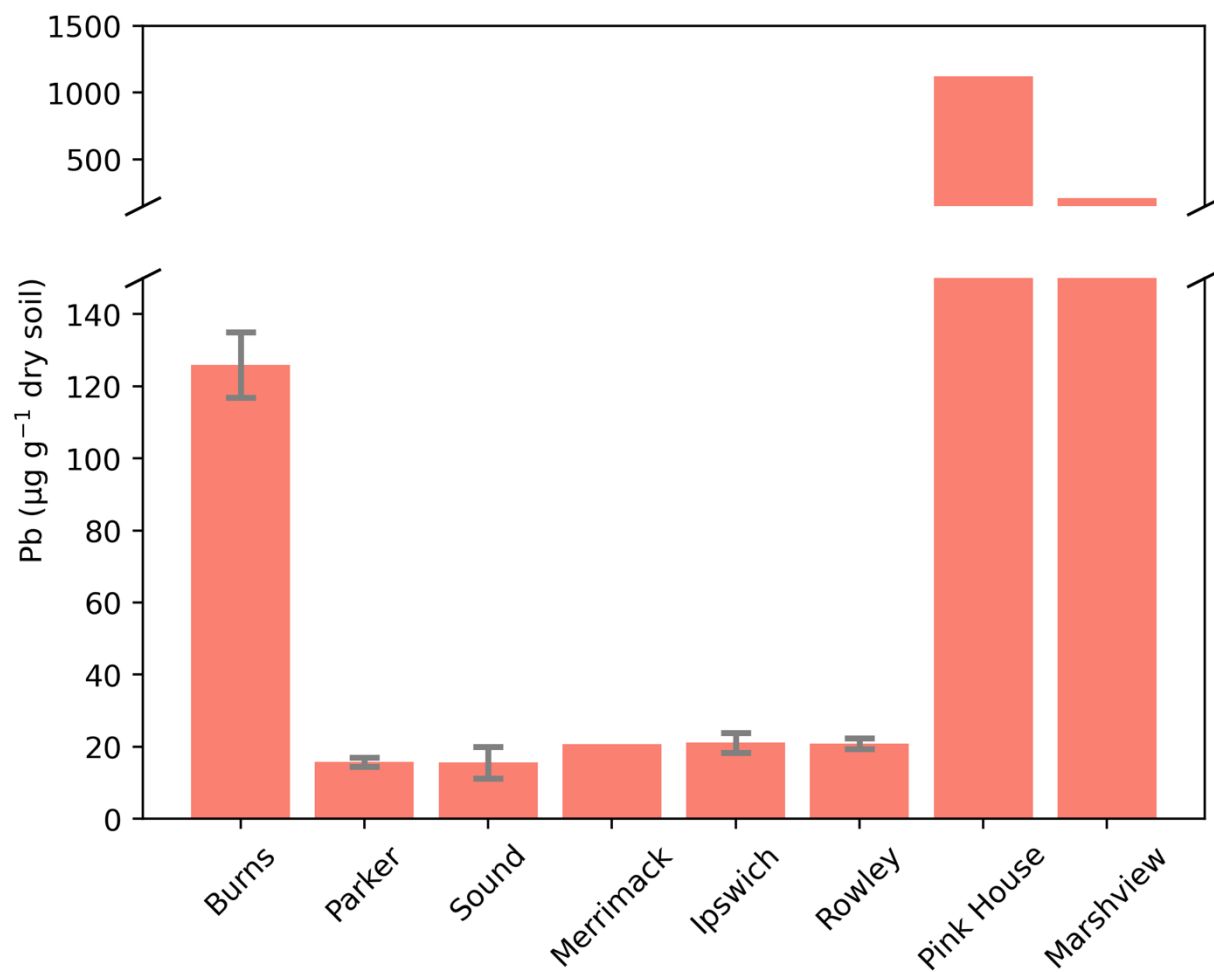


FIG. 3. Concentration of lead in surficial samples aggregated by region.

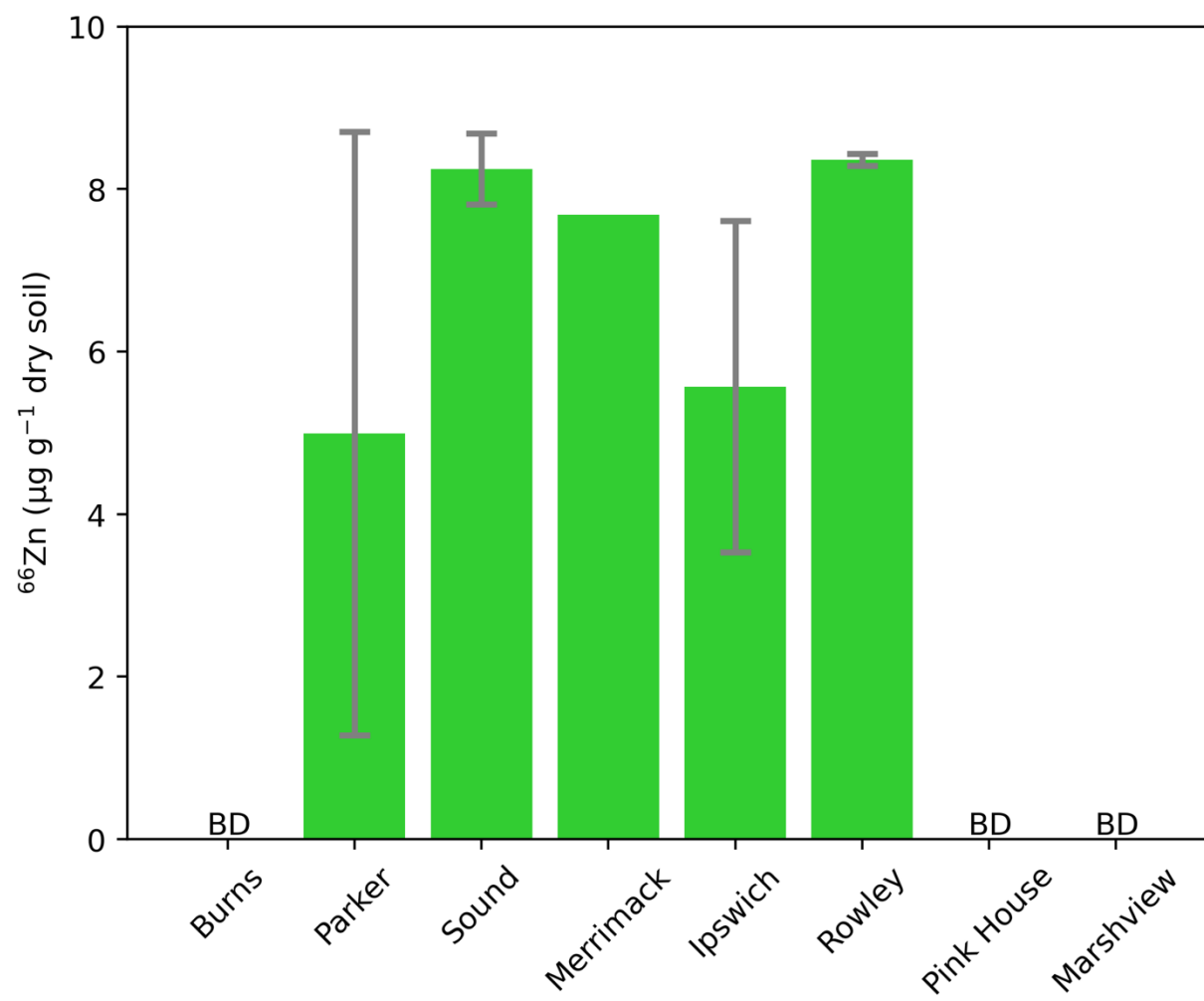


FIG. 4. Concentration of zinc-66 in surficial samples aggregated by region.

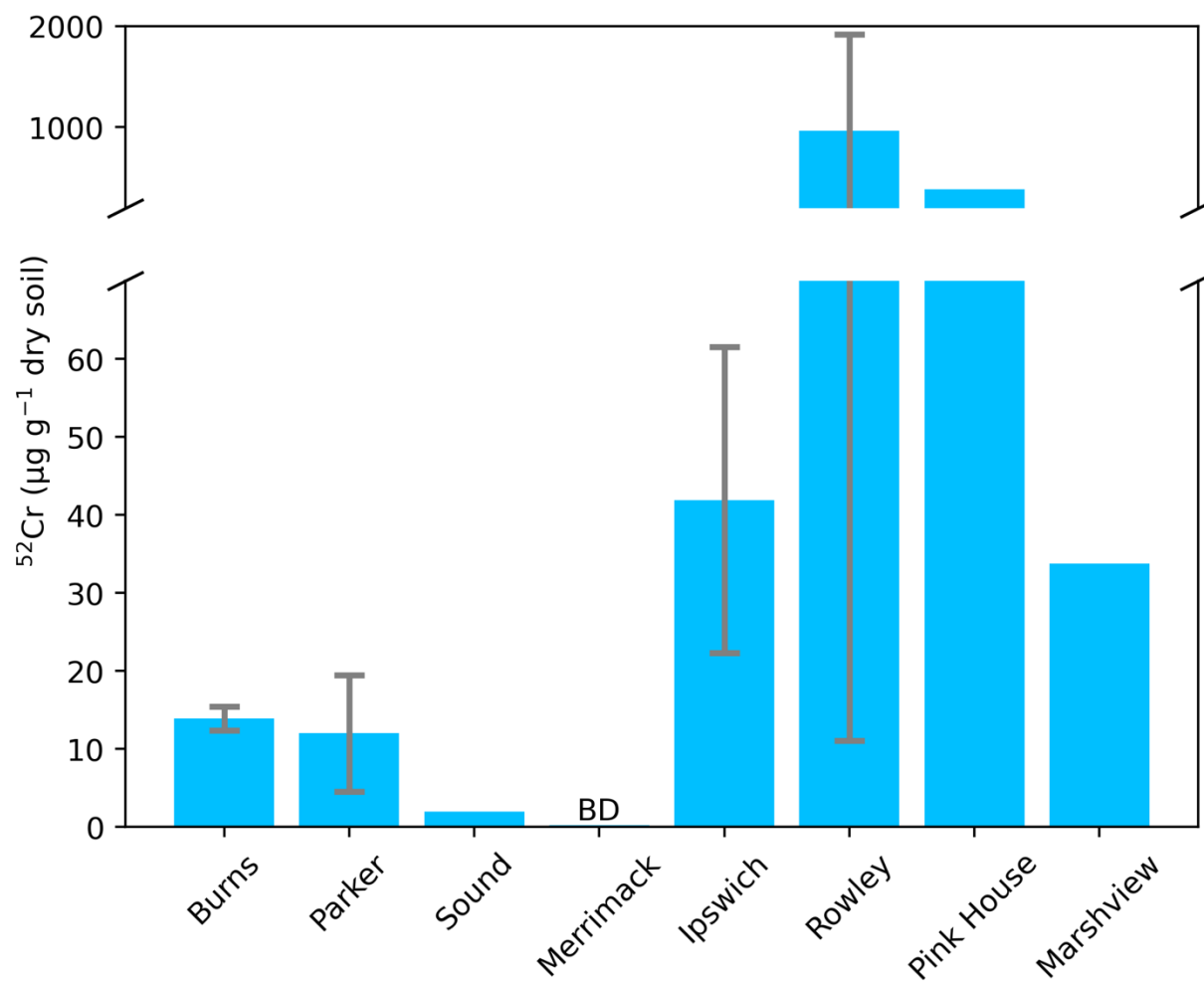


FIG. 5. Concentration of chromium-52 in surficial samples aggregated by region.

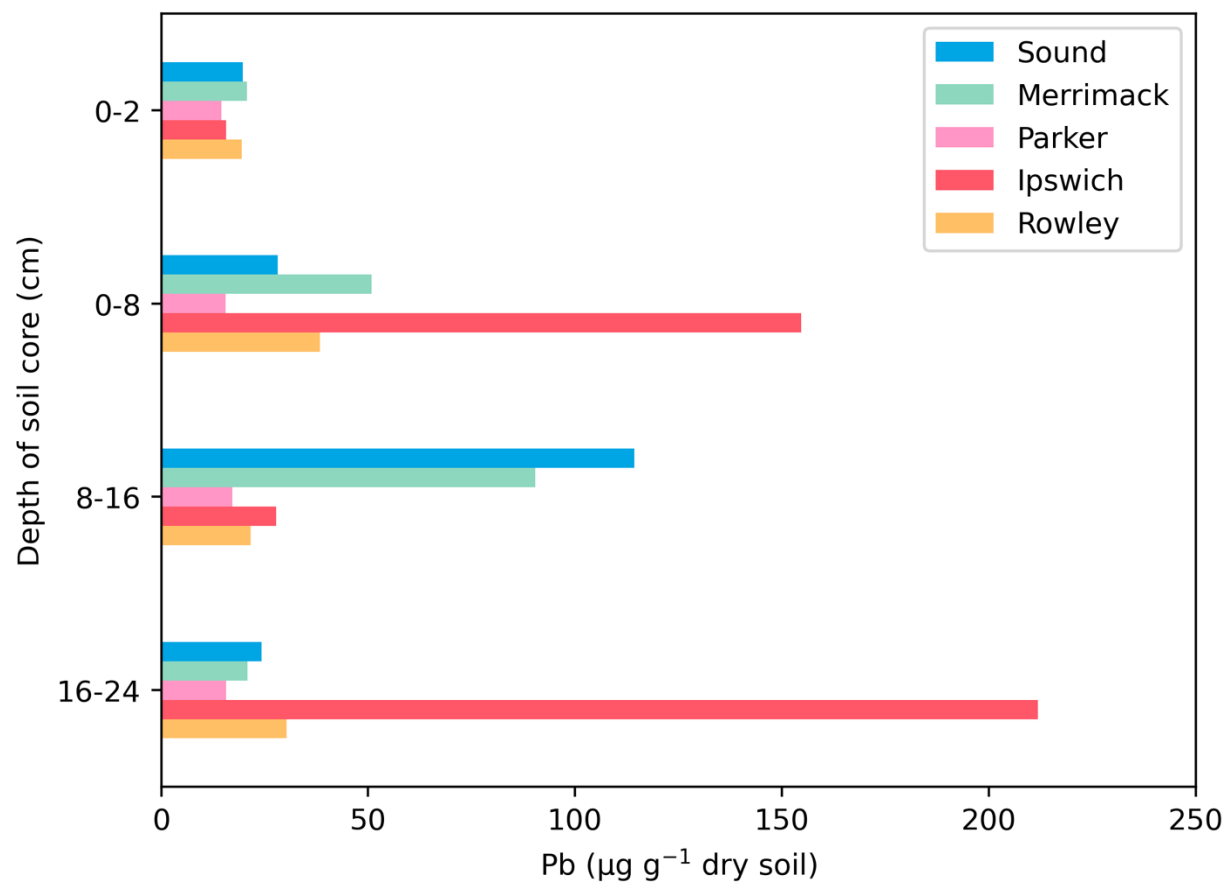


FIG. 6. Concentration of lead in core samples by depth.

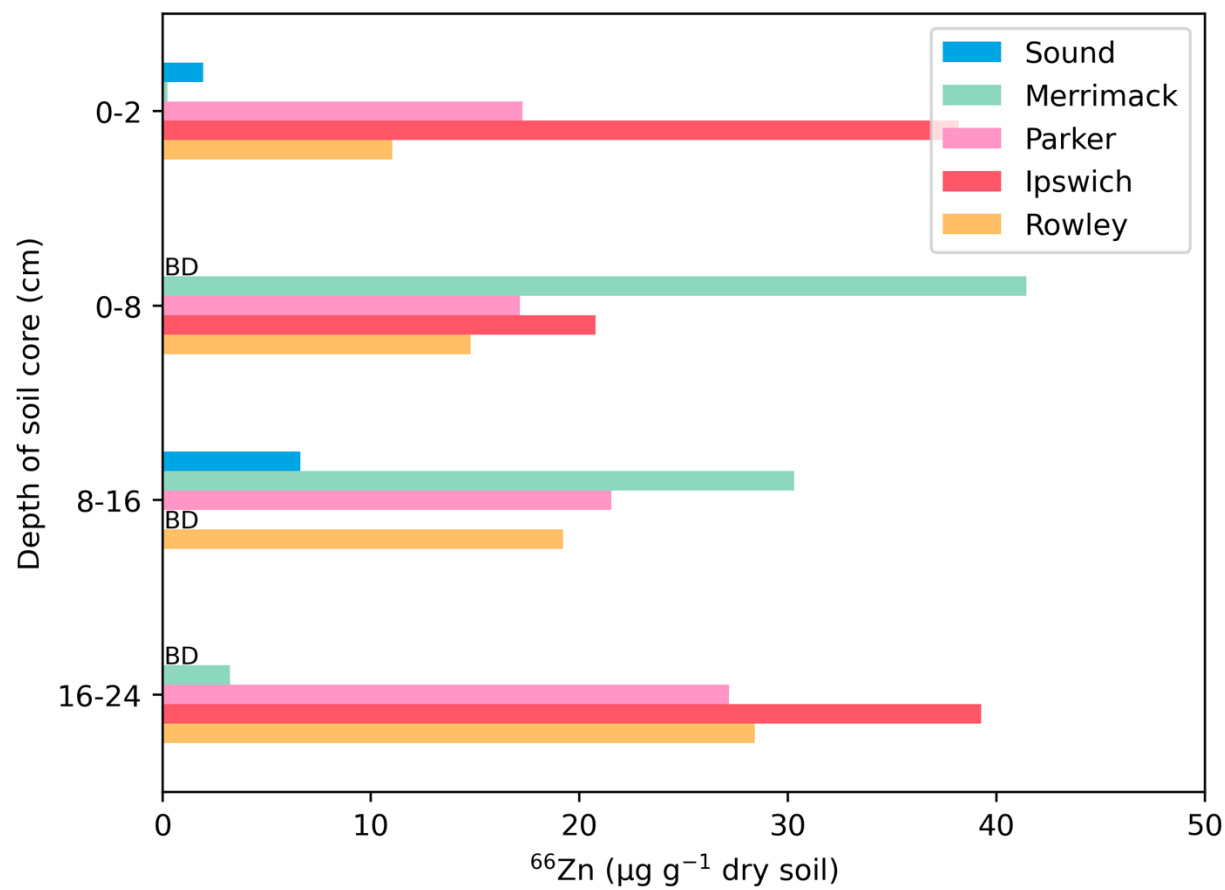


FIG. 7. Concentration of zinc-66 in core samples by depth.

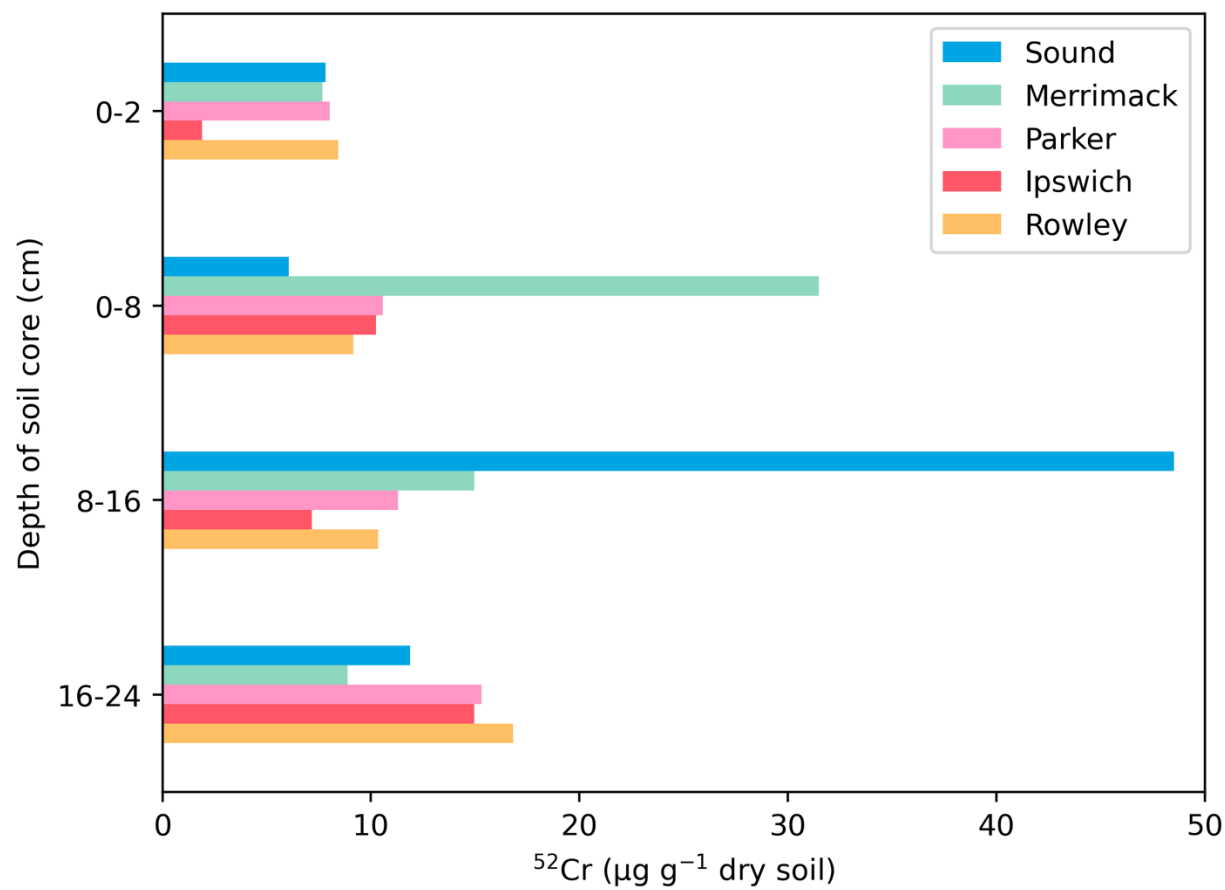


FIG. 8. Concentration of chromium-52 in core samples by depth.

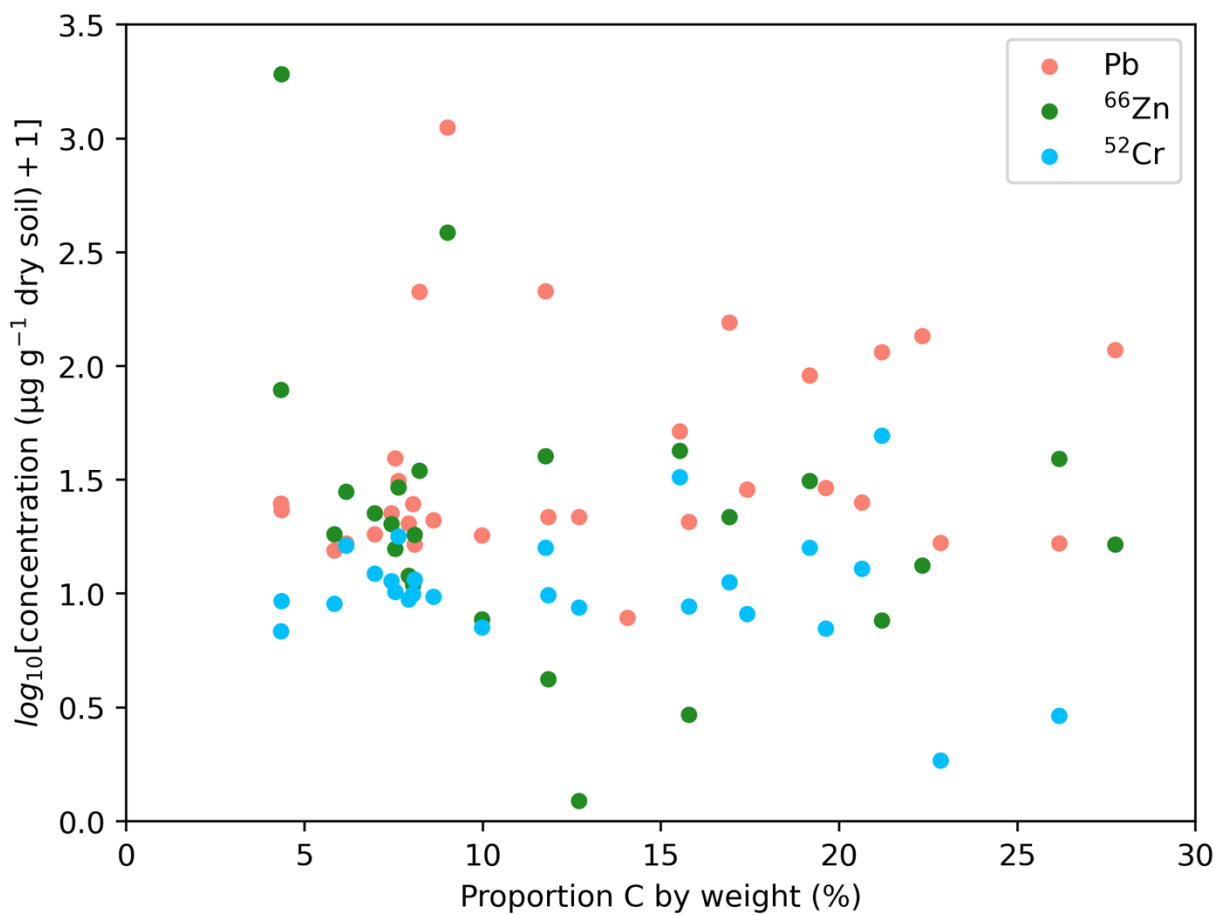


FIG. 9. Proportion carbon by weight versus log-transformed heavy metal concentration.

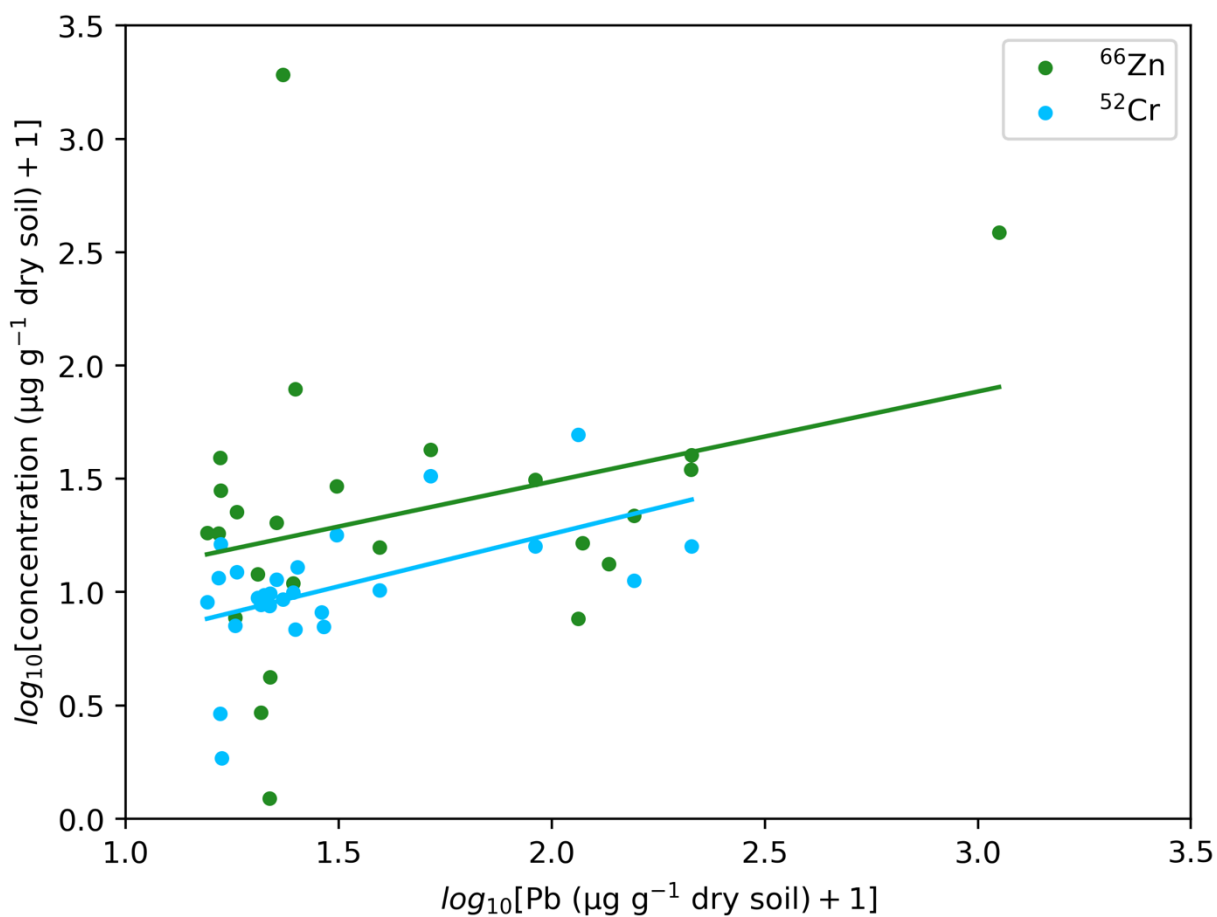


FIG. 10. Zinc-66 and log-transformed chromium-52 concentrations versus lead concentration, all log-transformed.

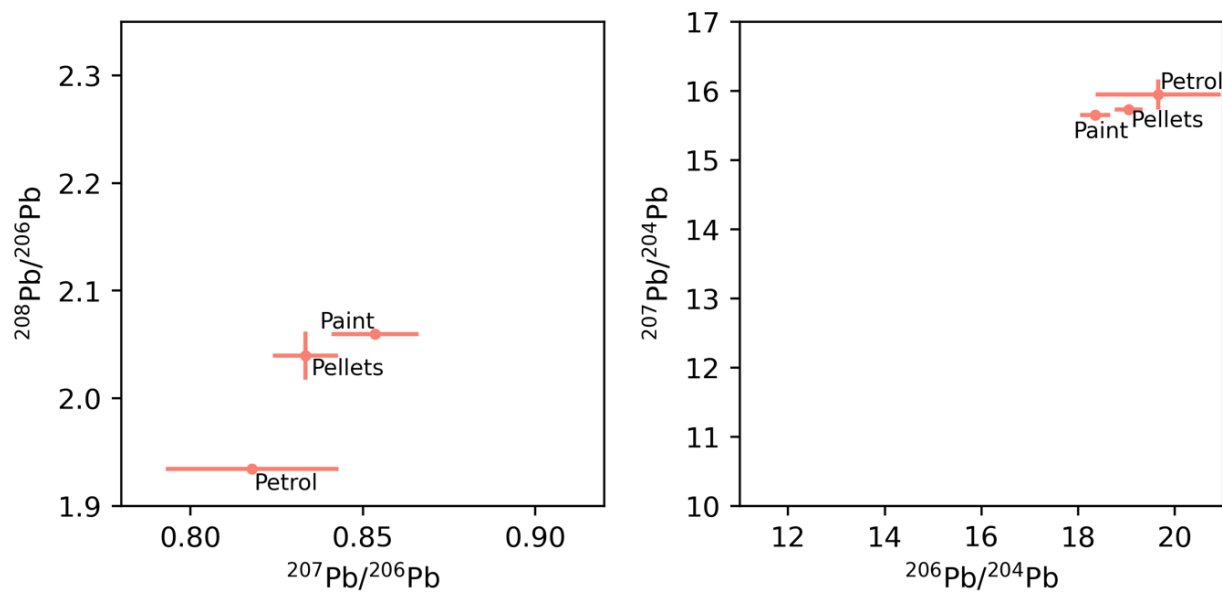


FIG. 11. Average endmember lead isotope ratios obtained from the scientific literature. See TABLE 2 for a list of primary sources consulted.

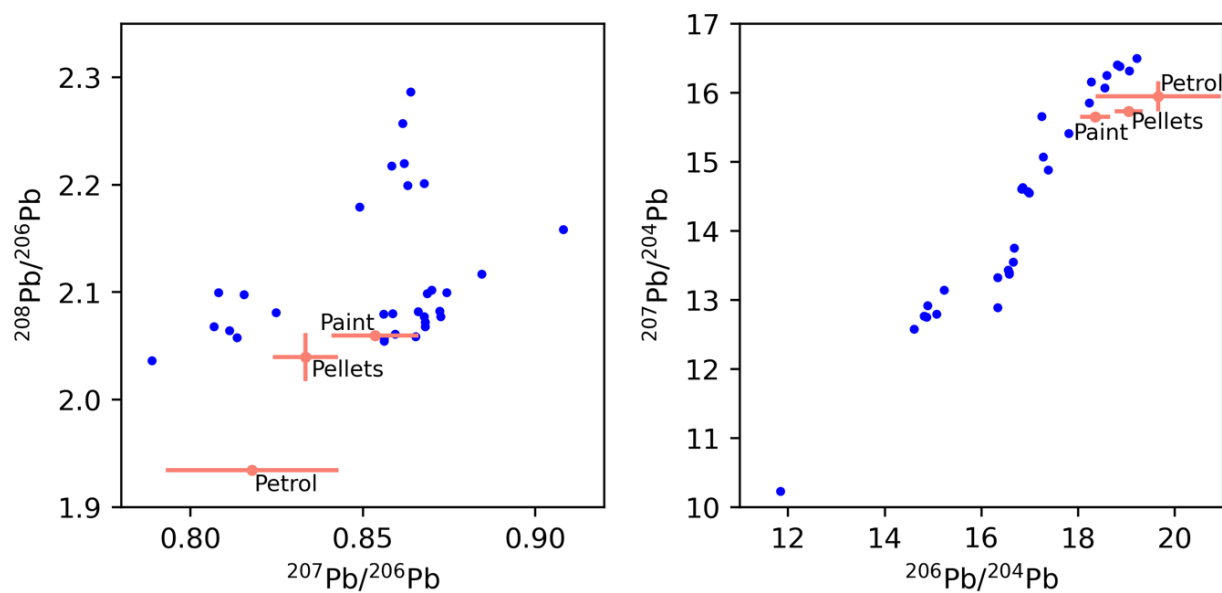


FIG. 12. Measured lead isotope ratios (blue) juxtaposed to those of presumed endmembers.

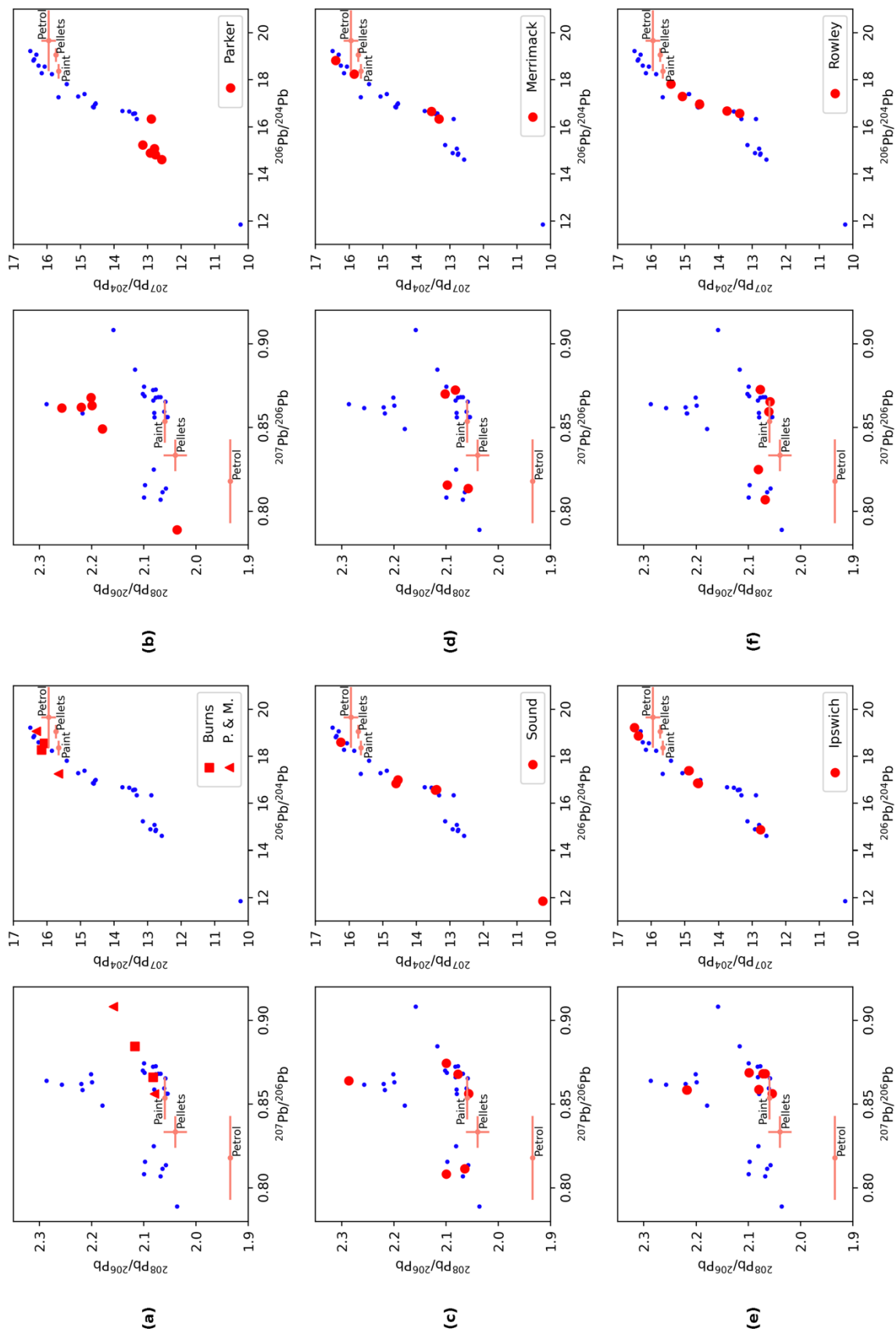


FIG. 13. Selected measured lead isotope ratios (red) juxtaposed to those of other measurements (blue) and of presumed endmembers:

(a) Burns plus Pink House and Marshview (P. & M.) (b) Parker (c) Sound (d) Merrimack (e) Ipswich (f) Rowley.

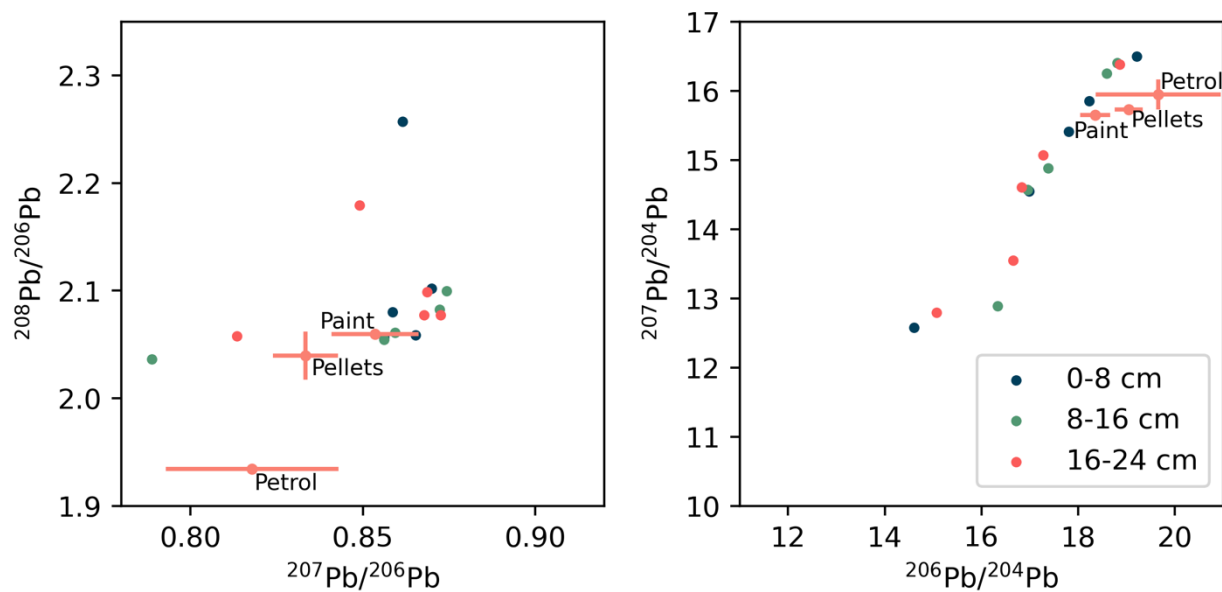


FIG. 14. Measured lead isotope ratios of cores juxtaposed to those of presumed endmembers.

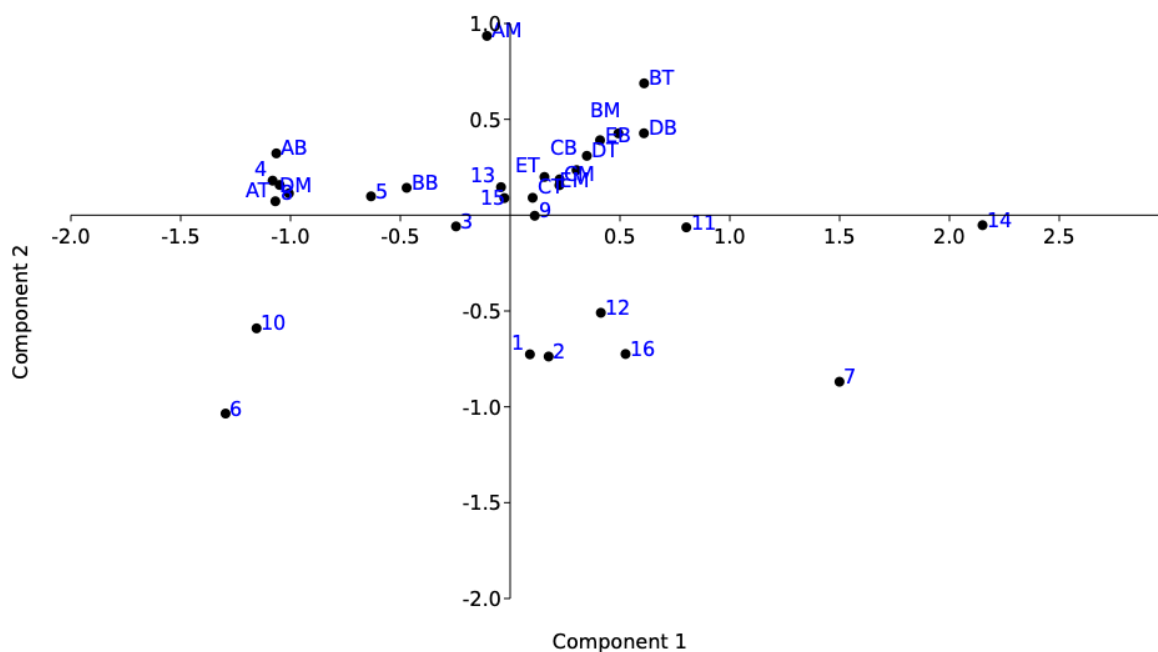


FIG. 15. Principal component analysis based on lead isotope ratios, zinc-66 and chromium-52 concentrations, and proportion carbon by weight. See TABLE 3 for further specifications.